# Performance of Distributed MISO Systems Using Cooperative Transmission with Antenna Selection

Jonghyun Park, Jaewon Kim, and Wonjin Sung

*Abstract:* **Performance of downlink transmission strategies exploiting cooperative transmit diversity is investigated for distributed multiple-input single-output (MISO) systems, for which geographically distributed remote antennas (RA) in a cell can either communicate with distinct mobile stations (MS) or cooperate for a common MS. Statistical characteristics in terms of the signal-to-interference-plus-noise ratio (SINR) and the achievable capacity are analyzed for both cooperative and non-cooperative transmission schemes, and the preferred mode of operation for given channel conditions is presented using the analysis result. In particular, we determine an exact amount of the maximum achievable gain in capacity when RAs for signal transmission are selected based on the instantaneous channel condition, by deriving a general expression for the SINR of such antenna selection based transmission. For important special cases of selecting a single RA for non-cooperative transmission and selecting two RAs for cooperative transmission among three RAs surrounding the MS, closed-form formulas are presented for the SINR and capacity distributions.**

*Index Terms:* **Antenna selection, capacity, cooperative transmission, distributed multiple-input multiple-output (MIMO), fading channels, transmit diversity.**

## I. INTRODUCTION

There has been a growing interest in using cooperative transmission (CT) in wireless systems due to its effectiveness of introducing spatial diversity. Such network coordination has been demonstrated to provide an increased capacity for various types of wireless cellular systems [1]–[4], including code division multiple access cellular [5]–[9] and sensor networks [10]. CT can be especially useful in reducing the outage probability of the system by enhancing the signal-to-interference-plus-noise ratio (SINR) of mobile stations (MS) which are marginally covered by a single remote antenna (RA). As one of efficient means to implement CT, systems utilizing distributed antennas have been investigated in [11]–[18]. Unlike systems employing user cooperation diversity [19]–[21], distributed antenna systems have multiple RAs which are wireline connected to each base station (BS), thus requiring no additional radio resources for relaying.

When each RA uses the same amount of power for transmission, CT always exhibits improved SINR performance over non-cooperative transmission (NCT) regardless of channel conditions [22], [23]. For the overall system capacity enhancement, however, CT needs to be performed selectively due to its duplicated usage of the spectrum resources, i.e., utilization of two RAs is justified only when the average capacity per radio unit exceeds the NCT capacity. Thus, an effective transmission strategy exploiting cooperative transmit diversity is desired to achieve the system capacity improvement. More specifically, for the MS located close to a certain RA, NCT can be a preferable mode of operation, whereas for the MS near the coverage boundary among RAs, CT can provide an increased bandwidth efficiency. This trade-off between the NCT and CT modes has been analyzed for soft handover techniques [7]–[9] and for the outage probability reduction [23].

In this work, the performance of distributed antenna transmission from multiple RAs to a target MS using both cooperative and non-cooperative modes of operation is investigated, in the view of capacity maximization. Frequency reuse 1 is assumed for the signal transmission from each RA, which either transmits the desired signal to the MS in a non-cooperative manner or cooperates with another RA for the signal quality enhancement. The remainder of the RAs in the system act as sources of interference. Cooperation methods in consideration are space-time block coding (STBC) [24] for open-loop cooperation, and STBC with channel state information (CSI) available at the transmitter [25] (referred to as STBC-T), equal gain transmission (EGT) [26], and maximum ratio transmission (MRT) [27] for closed-loop cooperations. Using these methods, we determine the preferred mode of operation for given channel conditions by presenting the statistical characteristics of the received signal quality as well as the corresponding spectral efficiency, and also quantify the amount of gain when adaptive transmission (AT) between the NCT and CT modes is performed.

Although such an adaptive operation enhances the transmission performance, an additional gain is expected if the MS located near RA coverage boundaries is served by different RAs (or different pairs of cooperating RAs) in a time-varying manner, via selection of RAs providing the maximum instantaneous SINR. In this scenario, each RA can either act as a desired signal source or an interference source at a particular instance, thus an exact analysis of the maximum SINR involves variables that are highly correlated. Due to this difficulty, existing results for the performance analysis of macroscopic diversity channels either use the independency assumption among component variables [28], [29], given correlation measures [30]–[32], Gaussian approximation for the interference [17], or simulation results [5].

Main contributions of this paper are the determination of exact distributions for SINR and capacity when RAs for signal transmission are selected based on instantaneous channel conditions, and corresponding quantification of the performance gain over conventional transmission methods for both cooperative and non-cooperative cases. In particular, a general expression

Manuscript received November 19, 2007.

The authors are with the Department of Electronic Engineering, Sogang University, Seoul, 121-742, Korea, email: {parkcrom, voch81, wsung}@sogang.ac.kr.

This work has been supported in part by the Telecommunications R&D Center, Samsung Electronics, and in part by the Special Research Grant of Sogang University.

for the maximum SINR distribution is derived first, which is applied to obtain closed-form formulas for important special cases.

The organization of the paper is as follows. The system and signal models as well as parameters used for the numerical evaluation are described in Section II. Cooperative and non-cooperative transmission methods and their SINR expressions are discussed in Section III for both cases with and without RA selection. Statistical characteristics of various transmission schemes in consideration are investigated in Section IV, where the cumulative distribution functions (CDF) for the SINR and the capacity are presented. In Section V, we compare the derived performance of transmission schemes and quantify the gain achieved by the RA selection. Finally, conclusions are given in Section VI.

## II. SYSTEM MODEL

Consider a distributed multiple-input single-output (MISO) system as described in Fig. 1, where the BS is wireline connected with 7 RAs geographically spread over the cell. A similar antenna structure is also used in adjacent cells. The RAs transmit signals with equal power over independent channels sharing the same radio resource, causing interference to each other. Assuming the total number of active RAs transmitting either desired or undesired signals to a target MS is $M$, the discrete-time received signal for the MS is given by

$$y = \sum_{i=1}^{M} \frac{h_i}{\sqrt{d_i^{\alpha}}} x_i + z \tag{1}$$

where $x_i$ is the transmit signal from RA $i$, $h_i$ is independent and identically distributed complex Gaussian variable with unit variance representing flat Rayleigh fading, and $z$ is the additive Gaussian noise with variance $\sigma_z^2$. Also, $d_i$ is the distance between RA $i$ and the MS, and $\alpha$ is the pathloss exponent.

Let us consider $L$ RAs in the center cell which are closest to the target MS, transmitting signals with significant power to the MS. While the value of $L$ can range from 1 to 7, a typical value in consideration is $L = 3$, as illustrated by RAs 1, 2, and 3 which surround the MS shown in Fig. 1. Let $S$ denote the number of RAs among $L$ significant transmission sources, which cooperate to transmit the desired signal to the target MS. Thus, $S = 1$ and 2 represent the NCT and CT, respectively. For the $n$th combination out of $\binom{L}{S}$, let $\mathcal{D}_n$ and $\mathcal{I}_n$ denote the sets of indices representing the RAs transmitting the desired signal and the interference signal, respectively. Note the cardinalities of $\mathcal{D}_n$ and $\mathcal{I}_n$ are $S$ and $L - S$, respectively. Using this notation, the received signal can be rewritten as

$$y = \underbrace{\sum_{i\in\mathcal{D}_n} \frac{h_i}{\sqrt{d_i^{\alpha}}} x_i}_{\text{Desired signal}} + \underbrace{\sum_{j\in\mathcal{I}_n} \frac{h_j}{\sqrt{d_j^{\alpha}}} x_j + \overbrace{\sum_{k=L+1}^{M} \frac{h_k}{\sqrt{d_k^{\alpha}}} x_k + z}^{\triangleq I}}_{\text{Undesired interference}} \tag{2}$$

where $I = z + \sum_{k=L+1}^{M} h_k x_k / \sqrt{d_k^{\alpha}}$ is the sum of the noise and the $M - L$ interference components. The received power becomes

$$\mathbb{E}[|y|^2] = \sum_{i\in\mathcal{D}_n} P_i + \sum_{j\in\mathcal{I}_n} P_j + \sigma_I^2 \tag{3}$$

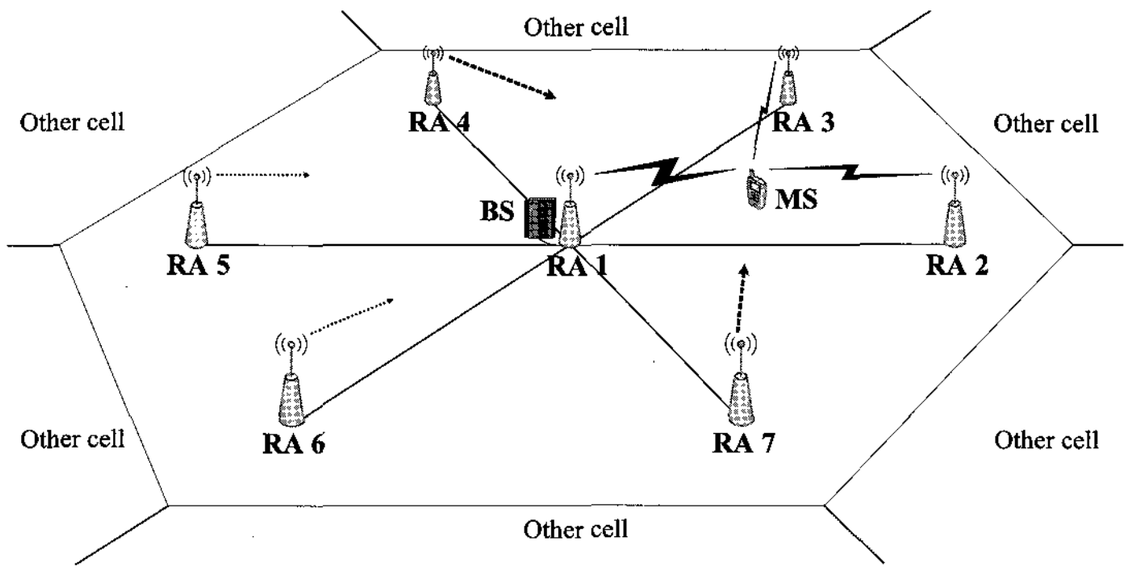


Fig. 1. An illustration of a distributed MISO system.

where $P_i = E_s|h_i|^2/d_i^{\alpha}$ is the signal power from RA $i$ with $E_s = \mathbb{E}[|x_i|^2]$, and $\sigma_I^2 = \mathbb{E}[|I|^2] = \sigma_z^2 + E_s \sum_{k=L+1}^{M} d_k^{-\alpha}$. We also define the average received power from RA $i$ as $\lambda_i = \mathbb{E}[P_i] = E_s/d_i^{\alpha}$, $i = 1, \cdots, M$. For all numerical performance evaluations, a 7-cell structure with $M = 49$ RAs is used, and the shortest distance between two RAs, e.g., between RA 1 and RA 2 is set to be 500 m. The pathloss exponent value of $\alpha = 3.76$ suggested in [33] is used unless otherwise stated. The average transmit power is set to be $E_s = \mathbb{E}[|x_i|^2] = 43$ dBm, and the average noise power is $\sigma_z^2 = -104$ dBm, corresponding to 10 MHz transmission bandwidth. Perfect measurement of the CSI at the receiver is assumed as well as the accurate knowledge of CSI at the transmitter for the closed-loop operation of CT.

## III. TRANSMISSION STRATEGIES

### A. Without RA Selection

For transmission without RA selection, we assume the RAs transmitting the desired signal are determined based on the average received power $\lambda_i$s and are not changed based on the instantaneous channel condition. Therefore, the RA corresponding to the largest value of $\lambda_i$ is the desired transmission source for the NCT mode, and the two RAs corresponding to the largest and second-largest $\lambda_i$s are the desired transmission sources for the CT mode. Transmission characteristics are presented and compared for the case of $L = 3$. Without loss of generality, we assume $\lambda_1 \geq \lambda_2 \geq \lambda_3$. Generalization to $L > 3$ cases is straightforward and is not included here. As will be shown, analysis based on $L = 3$ RAs surrounding the MS is sufficiently accurate.

#### A.1 Non-Cooperative Transmission

In conventional non-cooperative mode, transmission of the desired signal is performed by a single RA. For the MS communicating with RA 1, the SINR expression is given as

$$\gamma_{\text{NCT}} = \frac{P_1}{P_2 + P_3 + \sigma_I^2}. \tag{4}$$

The SINR becomes higher as the MS approaches to RA 1, and NCT is the preferred mode of transmission when the received power from a specific RA is dominant.

## A.2 Cooperative Transmission

Cooperation among RAs can be performed in either open-loop or closed-loop operations depending on the availability of the CSI. For the open-loop operation, STBC is considered, followed by STBC-T, EGT, and MRT for the closed-loop operation. Except the STBC with constant power allocation, other transmission schemes require some information of the channel at the transmitter as described below.

**STBC:** Alamouti's STBC for two transmit antennas and one receive antenna [24] can be applied for the CT from two RAs. The received signal vector $\mathbf{y} = [y_k \quad y_{k+1}]$ over two consecutive symbol periods over the MISO channel $\mathbf{g} = [g_1 \quad g_2] = [h_1/\sqrt{d_1^\alpha} \quad h_2/\sqrt{d_2^\alpha}]$ is expressed as $\mathbf{y} = \mathbf{gX} + \tilde{\mathbf{I}}$, for which $\mathbf{X}$ is the space-time codeword matrix and $\tilde{\mathbf{I}} = [\tilde{I}_k \quad \tilde{I}_{k+1}]$ is the undesired interference vector with $\mathbb{E}[|\tilde{I}_k|^2] = \mathbb{E}[|\tilde{I}_{k+1}|^2] = P_3 + \sigma_I^2$. The instantaneous SINR of the STBC for distributed MISO systems can be determined as [34], [35]

$$\gamma_{\text{STBC}} = \frac{P_1 + P_2}{P_3 + \sigma_I^2}. \tag{5}$$

**STBC-T:** The performance of STBC transmission can be improved by multiplying the channel conjugate vector to the transmission symbols when the channel information is available at the transmitter [25]. The received signal vector for STBC-T is written as $\mathbf{y} = \mathbf{gW}_{\text{STBC-T}}\mathbf{X} + \tilde{\mathbf{I}}$, where $\mathbf{W}_{\text{STBC-T}}$ is the diagonal weighting matrix whose diagonal elements are respectively $\sqrt{2}g_1^*/\|\mathbf{g}\|$ and $\sqrt{2}g_2^*/\|\mathbf{g}\|$. The SINR expression can be determined in a similar manner to the STBC case [34] as

$$\gamma_{\text{STBC-T}} = \frac{2(P_1^2 + P_2^2)}{(P_1 + P_2)(P_3 + \sigma_I^2)}. \tag{6}$$

**EGT:** By coherently adjusting the phases of the transmission signals using weighting vector $\mathbf{w}_{\text{EGT}} = [g_1^*/|g_1| \quad g_2^*/|g_2|]^T$ with constant power allocation among RAs [26], the received signal for the EGT mode becomes $y = \mathbf{gw}_{\text{EGT}}x + \tilde{I}$, where $x$ is the common transmission symbol from RA 1 and RA 2, and $\tilde{I}$ is the interference component with its average power $\mathbb{E}[|\tilde{I}|^2] = P_3 + \sigma_I^2$. The SINR for EGT is

$$\gamma_{\text{EGT}} = \frac{(\sqrt{P_1} + \sqrt{P_2})^2}{P_3 + \sigma_I^2}. \tag{7}$$

**MRT:** For maximization of the receiver SINR, weighting vector $\mathbf{w}_{\text{MRT}} = [\sqrt{2}g_1^*/\|\mathbf{g}\| \quad \sqrt{2}g_2^*/\|\mathbf{g}\|]^T$ matched to channel $\mathbf{g}$ is multiplied to the common transmission symbol $x$ from RA 1 and RA 2. The received signal in this case is written as $y = \mathbf{gw}_{\text{MRT}}x + \tilde{I}$. The SINR for MRT in distributed MISO systems can be similarly determined as the SINR for conventional MRT in [27] as

$$\gamma_{\text{MRT}} = \frac{2(P_1 + P_2)}{P_3 + \sigma_I^2}. \tag{8}$$

We observe 3 dB SINR gain of MRT over STBC from the relation $\gamma_{\text{MRT}} = 2\gamma_{\text{STBC}}$. Note STBC-T and MRT allocate different power levels to different antennas based on instantaneous channel conditions, thus appropriate transmit power adjustment capability is needed for the system.

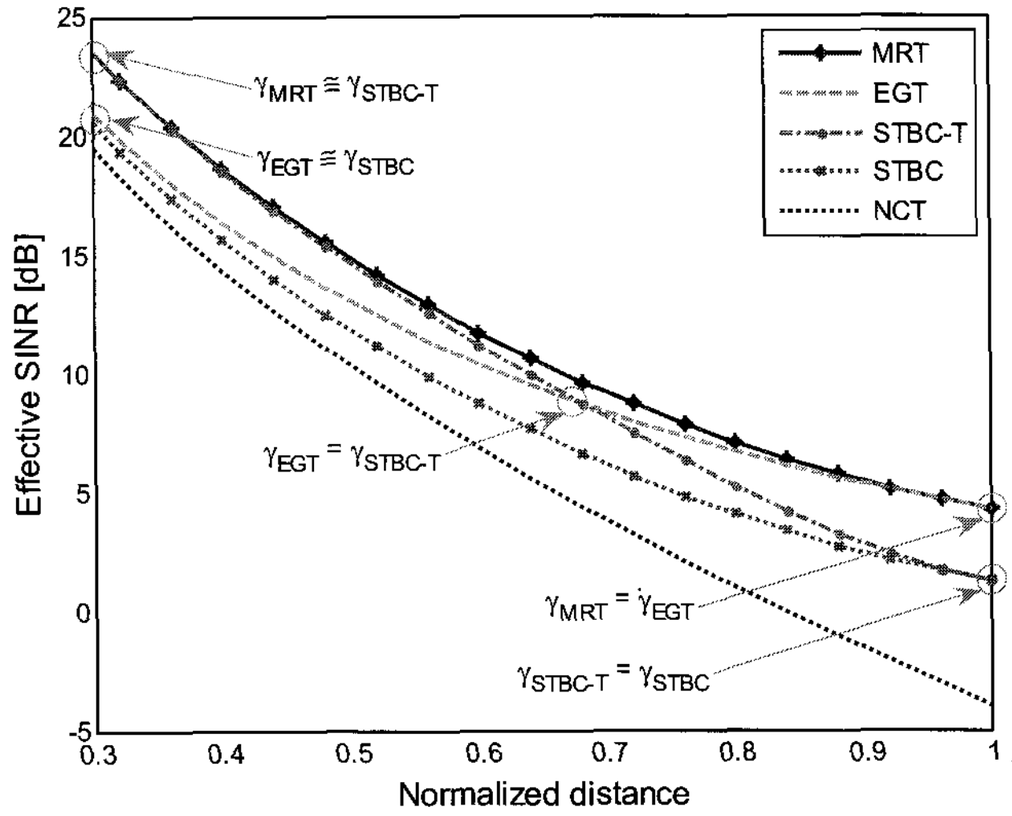


Fig. 2. Comparison of effective SINR values among the transmission schemes for varying locations of the target MS from RA 1 (normalized distance 0) to the center point among RAs 1, 2, and 3 (normalized distance 1).

The SINR of five different transmission modes are plotted and compared using the static channel condition $h_i = 1$ in Fig. 2, where the horizontal axis represents the location of the MS which moves along the straight line connecting RA 1 (denoted as normalized distance of 0) and the center point among RAs 1, 2, and 3 (denoted as normalized distance of 1). RA 1 is the desired signal source for NCT. Also, RAs 1 and 2 are the desired signal sources for CT modes. As the normalized distance increases from 0 to 1, the amount of interference increases while the desired signal power becomes reduced, thus resulting in decreasing values of SINR. In terms of SINR, NCT is outperformed by all four CT modes in consideration, among which the open-loop STBC and closed-loop MRT modes respectively exhibit the lowest and highest SINR over the entire range of the normalized distance. The SINR curves for EGT and STBC-T lie between those for STBC and MRT, and crosses at normalized distance value of 0.68; EGT outperforms STBC-T and approaches to the MRT performance as the distance increases to 1, while STBC-T outperforms EGT and approaches to the MRT performance as the distance decreases to 0. For the remainder of our discussion on cooperation between RAs, we only consider MRT with the best SINR performance among CT modes, and define $\gamma_{\text{CT}} \triangleq \gamma_{\text{MRT}}$.

## A.3 Adaptive Transmission

Although CT demonstrates higher SINR values than that of NCT, this does not necessarily imply CT is always the preferred mode of operation for systems with distributed RAs in terms of maximizing the overall data rate, since CT consumes twice the radio resource than NCT does. With the fully loaded traffic, two RAs can either serve two distinct MSs or one common MS. Hence the usage of CT is justified when the SINR gain over NCT is large enough to compensate for the duplicated resource utilization. We define the capacity for NCT and CT normalized by the bandwidth and the number of radio units as

$$\phi_{\text{NCT}} = \log_2(1 + \gamma_{\text{NCT}}) \tag{9}$$

and

$$\phi_{\text{CT}} = \frac{1}{2}\log_2(1+\gamma_{\text{CT}}) \tag{10}$$

with the unit of [bps/Hz/RA] which represents the bandwidth efficiency per RA, i.e., the normalization factor of $1/2$ is used for $\phi_{\text{CT}}$ to account for the utilization of two RAs.

In the adaptive cooperation mode, either NCT or CT is used among the RAs based on the instantaneous channel condition so as to maximize the normalized capacity. Thus, NCT is performed when $\phi_{\text{NCT}} > \phi_{\text{CT}}$ or equivalently

$$\gamma_{\text{NCT}} > \sqrt{\gamma_{\text{CT}}+1} - 1$$

and CT is performed otherwise. The capacity of AT for a given channel condition is defined as

$$\phi_{\text{AT}} = \max(\phi_{\text{NCT}}, \phi_{\text{CT}}). \tag{11}$$

*B. With RA Selection*

Further capacity improvement is expected when RAs transmitting the desired signal to the target MS are selected based on the instantaneous channel conditions, not based on the average received power. This is especially the case for the MS located near RA coverage boundaries, since the signals from some of the RAs are transmitted in more favorable channel conditions than others at certain time periods. Using the notation in Section II, the SINR for the MS receiving its desired signal from $S$ sources out of $L$ significant sources is defined as

$$\gamma_n^{(L,S)} = \frac{\sum_{i\in\mathcal{D}_n} P_i}{\sum_{j\in\mathcal{I}_n} P_j + \sigma_I^2} \tag{12}$$

for the $n$th combination out of $\binom{L}{S} \triangleq N$. Let $m$ be the index satisfying $m = \text{argmax}\{\gamma_n^{(L,S)}\}$ for $1 \le n \le N$. Then, the maximum SINR for the transmission with RA selection is denoted by

$$\Gamma_{\max}^{(L,S)} = \gamma_m^{(L,S)}. \tag{13}$$

B.1 NCT-RAS

RA selection can be performed for all of NCT, CT, and AT modes. In the case of the NCT mode, an RA transmitting the desired signal is chosen from $L = 3$ candidate RAs. The maximum SINR for *non-cooperative transmission with RA selection* (NCT-RAS), denoted as $\Gamma_{\text{NCT}}$ is

$$\begin{aligned}\Gamma_{\text{NCT}} &= \Gamma_{\max}^{(3,1)} \\ &= \max\left\{\frac{P_1}{P_2+P_3+\sigma_I^2}, \frac{P_2}{P_3+P_1+\sigma_I^2}, \frac{P_3}{P_1+P_2+\sigma_I^2}\right\}\end{aligned} \tag{14}$$

and the corresponding normalized capacity is determined as

$$\Phi_{\text{NCT}} = \log_2(1+\Gamma_{\text{NCT}}) \tag{15}$$

which represents the maximum achievable bandwidth efficiency when NCT-RAS is used.

B.2 CT-RAS

In the CT mode, three options exist for the selection of two cooperating RAs from three RAs with significant received power at the MS. By denoting the maximum SINR for *cooperative transmission with RA selection* (CT-RAS) as $\Gamma_{\text{CT}}$, we have

$$\begin{aligned}\Gamma_{\text{CT}} &= 2\Gamma_{\max}^{(3,2)} \\ &= \max\left\{\frac{2(P_1+P_2)}{P_3+\sigma_I^2}, \frac{2(P_2+P_3)}{P_1+\sigma_I^2}, \frac{2(P_3+P_1)}{P_2+\sigma_I^2}\right\}\end{aligned} \tag{16}$$

where the multiplication factor of 2 represents the SINR gain of MRT as identified in (8). The normalized capacity for this case is expressed as

$$\Phi_{\text{CT}} = \frac{1}{2}\log_2(1+\Gamma_{\text{CT}}). \tag{17}$$

B.3 AT-RAS

Transmission can be performed adaptively between NCT and CT while favorable RAs are selected at the same time. By comparing capacity values $\Phi_{\text{NCT}}$ and $\Phi_{\text{CT}}$, either NCT-RAS or CT-RAS is performed to achieve the maximum efficiency for the given channel condition. The capacity expression for *adaptive transmission with RA selection* (AT-RAS) is given by

$$\Phi_{\text{AT}} = \max(\Phi_{\text{NCT}}, \Phi_{\text{CT}}).$$

## IV. SINR AND CAPACITY DISTRIBUTIONS

Derivation procedures to obtain the CDFs of SINR and capacity are presented, which are applicable to any statistical channel models. For the Rayleigh fading channel model in consideration, we further provide closed-form expressions of CDFs. The received signal powers $P_1$, $P_2$, and $P_3$ over the Rayleigh fading channel are independent exponential random variables with respective means $\lambda_1$, $\lambda_2$, and $\lambda_3$ with the probability density function (pdf) given by

$$f_{P_i}(p) = \frac{1}{\lambda_i}e^{-\frac{p}{\lambda_i}} \tag{18}$$

for $p \ge 0$, and $f_{P_i}(p) = 0$ otherwise. Also, the pdf of the sum of two independent exponential random variables, e.g., $P_i + P_j$, is determined as [36]

$$f_{P_i+P_j}(p) = \begin{cases} \frac{p}{\lambda^2}e^{-\frac{p}{\lambda}}, & \text{if } \lambda_i = \lambda_j = \lambda \\ \frac{1}{\lambda_i-\lambda_j}\left(e^{-\frac{p}{\lambda_i}} - e^{-\frac{p}{\lambda_j}}\right), & \text{if } \lambda_i \ne \lambda_j \end{cases} \tag{19}$$

for $p \ge 0$, and $f_{P_i+P_j}(p) = 0$ otherwise.

*A. SINR Distributions: Without RA Selection*

Since $\gamma_{\text{NCT}}$ in (4) is the ratio of random variables, the pdf of $\gamma_{\text{NCT}}$ can be obtained by the transformation rule in [37, p. 141] as

$$f_{\gamma_{\text{NCT}}}(\gamma) = \int_{-\infty}^{\infty} f_{P_1,P_2+P_3+\sigma_I^2}(\gamma q, q)|q|dq. \tag{20}$$

Due to the statistical independence among $P_1$, $P_2$, and $P_3$, the pdf of $\gamma_{\text{NCT}}$ becomes

$$f_{\gamma_{\text{NCT}}}(\gamma) = \int_{\sigma_I^2}^{\infty} f_{P_1}(\gamma q) f_{P_2+P_3}(q-\sigma_I^2) q dq \tag{21}$$

where the integration interval of $q$ is determined from the range for which $f_{P_2+P_3}(q-\sigma_I^2)$ is not zero. The CDF of $\gamma_{\text{NCT}}$ is then obtained as

$$\begin{aligned} F_{\gamma_{\text{NCT}}}(\gamma) &= \int_0^{\gamma} f_{\gamma_{\text{NCT}}}(r)dr \\ &= \int_{\sigma_I^2}^{\infty} \left( \int_0^{\gamma} f_{P_1}(\underbrace{rq}_{\triangleq t})dr \right) f_{P_2+P_3}(q-\sigma_I^2)qdq \\ &= \int_{\sigma_I^2}^{\infty} \left( \int_0^{\gamma q} f_{P_1}(t)dt \right) f_{P_2+P_3}(q-\sigma_I^2)dq \\ &= 1 - \frac{e^{-\frac{\gamma\sigma_I^2}{\lambda_1}}\lambda_1^2}{(\lambda_1+\gamma\lambda_2)(\lambda_1+\gamma\lambda_3)} \end{aligned} \tag{22}$$

for $\gamma \geq 0$, and $F_{\gamma_{\text{NCT}}}(\gamma) = 0$ otherwise.

By following the similar procedure, the CDF of $\gamma_{\text{CT}}$ is derived as

$$\begin{aligned} F_{\gamma_{\text{CT}}}(\gamma) &= \int_{\sigma_I^2}^{\infty} \left( \int_0^{2\gamma q} f_{P_1+P_2}(t)dt \right) f_{P_3}(q-\sigma_I^2)dq \\ &= \begin{cases} 1 - \dfrac{4e^{-\frac{\gamma\sigma_I^2}{\lambda_1}}\left(\lambda_3\sigma_I^2\gamma^2 + \lambda_1(2\lambda_3+\sigma_I^2)\gamma + \lambda_1^2\right)}{(2\lambda_1+\gamma\lambda_3)^2}, \\ \qquad\qquad \text{if } \lambda_i = \lambda_j = \lambda \\ 1 - \dfrac{2}{(\lambda_1-\lambda_2)}\left\{ \dfrac{e^{-\frac{\gamma\sigma_I^2}{2\lambda_1}}\lambda_1^2}{(2\lambda_1+\gamma\lambda_3)} - \dfrac{e^{-\frac{\gamma\sigma_I^2}{2\lambda_2}}\lambda_2^2}{(2\lambda_2+\gamma\lambda_3)} \right\}, \\ \qquad\qquad \text{if } \lambda_i \neq \lambda_j \end{cases} \end{aligned} \tag{23}$$

for $\gamma \geq 0$, and $F_{\gamma_{\text{CT}}}(\gamma) = 0$ otherwise.

### *B. SINR Distributions: With RA Selection*

We define $U_n \triangleq \sum_{i\in\mathcal{D}_n} P_i$ and $V_n \triangleq \sum_{j\in\mathcal{I}_n} P_j + \sigma_I^2$, which are respectively the numerator and denominator in (12). Since $U_n$ and $V_n$ are the sums of independent random variables, the corresponding pdfs are obtained using generalized convolution integrals

$$f_{U_n}(u) = \prod_{i\in\mathcal{D}_n} \int_{a_i}^{b_i} f_{P_i}(p_i)dp_i \tag{24}$$

and

$$f_{V_n}(v) = \prod_{j\in\mathcal{I}_n} \int_{a_j}^{b_j} f_{P_j}(p_j)dp_j \tag{25}$$

where $[a_i, b_i]$ for $i \in \mathcal{D}_n$ denotes the range of integration variables satisfying $\sum_{i\in\mathcal{D}_n} p_i = u$, and $[a_j, b_j]$ for $j \in \mathcal{I}_n$ denotes the range of integration variables satisfying $\sum_{j\in\mathcal{I}_n} p_j + \sigma_I^2 = v$.

Let us assume the $n$th combination of the RAs produces the maximum SINR, i.e., $m = n$. By using the notation of the descending ordered variables $P_{(1)} \geq P_{(2)} \geq \cdots \geq P_{(L)}$ as in [38], $\gamma_n^{(L,S)}$ can be represented as

$$\gamma_n^{(L,S)} = \frac{U_n}{V_n} = \frac{\sum_{i\in\mathcal{D}_n} P_i}{\sum_{j\in\mathcal{I}_n} P_j + \sigma_I^2} = \frac{\sum_{i=1}^{S} P_{(i)}}{\sum_{j=S+1}^{L} P_{(j)} + \sigma_I^2}. \tag{26}$$

Note that the relation $P_i \geq P_{(S+1)}$ holds for all $i \in \mathcal{D}_n$. Thus, the conditional pdf $f_{U_n|V_n}(u|v)$ is equivalent to $f_{U_n}(u)$ except the additional constraint $p_i \geq p_{(S+1)}$ over $[a_i, b_i]$ for all $i \in \mathcal{D}_n$. From the relation $f_{U_n,V_n}(u,v) = f_{U_n|V_n}(u|v)f_{V_n}(v)$, the joint pdf is obtained as

$$f_{U_n,V_n}(u,v) = \prod_{k=1}^{L} \int_{a_k}^{b_k} f_{P_k}(p_k)dp_k \tag{27}$$

where $[a_k, b_k]$ denotes the range of integration variable $p_k$ satisfying the first condition

$$\sum_{i\in\mathcal{D}_n} p_i = u, \quad \sum_{j\in\mathcal{I}_n} p_j + \sigma_I^2 = v \tag{28}$$

and the second condition

$$p_i \geq p_{(S+1)} \text{ for } i \in \mathcal{D}_n. \tag{29}$$

Using the joint pdf in (27), the CDF of $\gamma_n^{(L,S)}$ is given by

$$\begin{aligned} \Pr\{\gamma_n^{(L,S)} \leq \gamma\} &= \Pr\left\{\frac{U_n}{V_n} \leq \gamma\right\} \\ &= \int_{\sigma_I^2}^{\infty} \Pr\{U_n \leq v\gamma, V_n = v\}dv \\ &= \int_{\sigma_I^2}^{\infty} \int_{Sp_{(S+1)}}^{v\gamma} f_{U_n,V_n}(u,v)dudv \end{aligned} \tag{30}$$

for $\gamma \geq 0$, where the integration over $u$ started from $Sp_{(S+1)}$ to satisfy the second condition given in (29). Since the CDF in (30) is nonnegative, the starting and ending points for the integration over $u$ should also satisfy the third condition

$$v\gamma \geq Sp_{(S+1)}. \tag{31}$$

The RA combination producing the maximum SINR can be any of $N$ combinations and such events are disjoint. Thus, the CDF for $\Gamma_{\text{max}}^{(L,S)}$ is determined as

$$\begin{aligned} F_{\Gamma_{\text{max}}^{(L,S)}}(\gamma) &= \sum_{n=1}^{N} \Pr\{\gamma_n^{(L,S)} \leq \gamma, m = n\} \\ &= \sum_{n=1}^{N} \int_{\sigma_I^2}^{\infty} \left[ \int_{Sp_{(S+1)}}^{v\gamma} f_{U_n,V_n}(u,v)du \right] dv \end{aligned} \tag{32}$$

for $\gamma \geq 0$ under the three conditions given in (28), (29), and (31), and $F_{\Gamma_{\text{max}}^{(L,S)}}(\gamma) = 0$ otherwise.

The general expression for $F_{\Gamma_{\text{max}}^{(L,S)}}(\gamma)$ in (32) can be applied to determine the CDF of the maximum SINR when $S$ out of $L$ RAs perform cooperative transmission over the channels with known power distributions. For NCT-RAS over the Rayleigh fading channel, the expression for the CDF of $\Gamma_{\text{NCT}}(=\Gamma_{\text{max}}^{(3,1)})$ is determined as

$$\begin{aligned} F_{\Gamma_{\text{NCT}}}(\gamma) &= F_{\Gamma_{\text{max}}^{(3,1)}}(\gamma) \\ &= \begin{cases} 1-\mu_1(\gamma), & \text{for } \gamma \geq 1 \\ 1-\mu_1(\gamma)-\mu_2(\gamma), & \text{for } \frac{1}{2} \leq \gamma < 1 \\ 1-\mu_1(\gamma)-\mu_2(\gamma)-\mu_3(\gamma), & \text{for } 0 \leq \gamma < \frac{1}{2} \\ 0, & \text{otherwise.} \end{cases} \end{aligned} \tag{33}$$

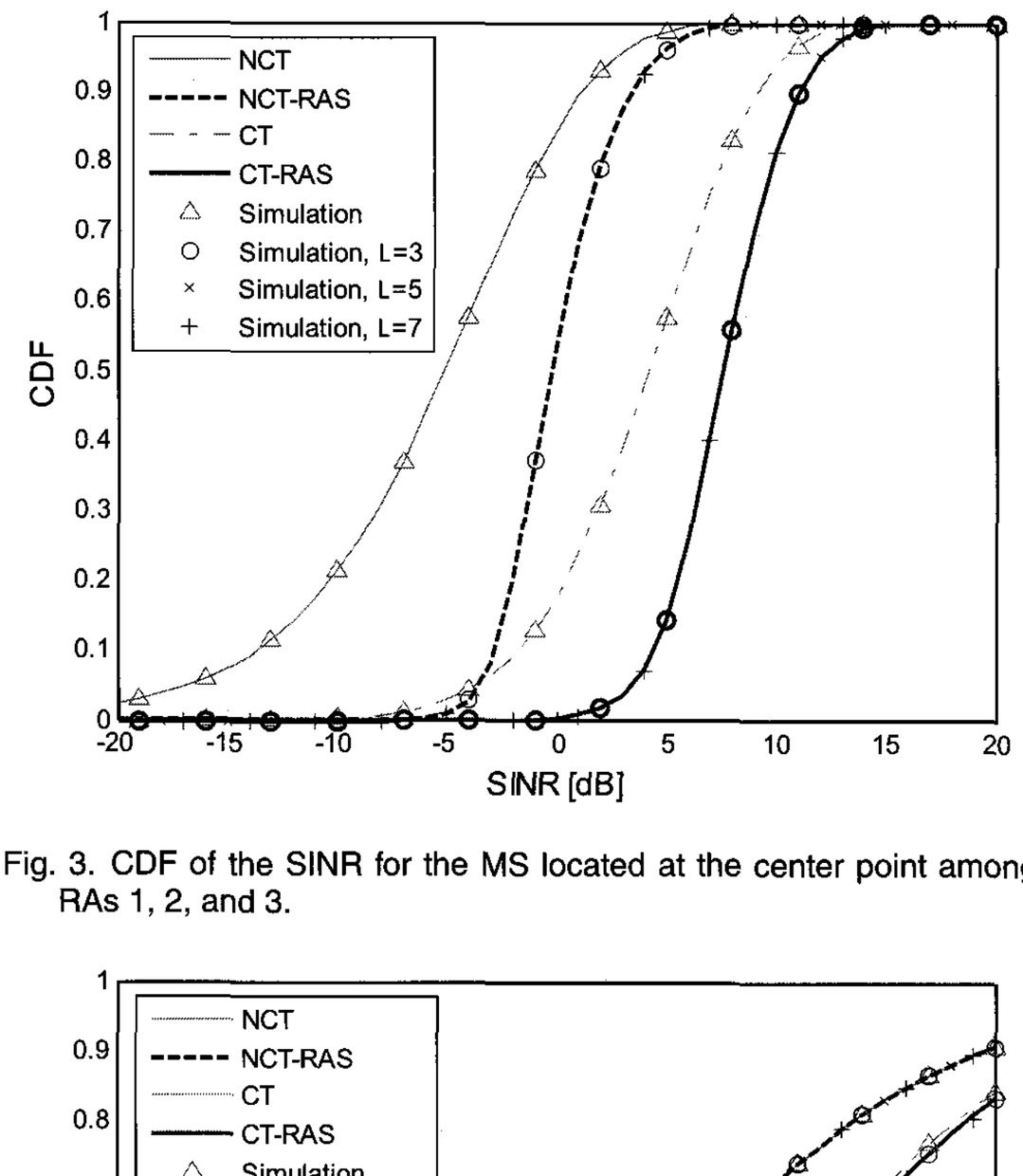


Fig. 3. CDF of the SINR for the MS located at the center point among RAs 1, 2, and 3.

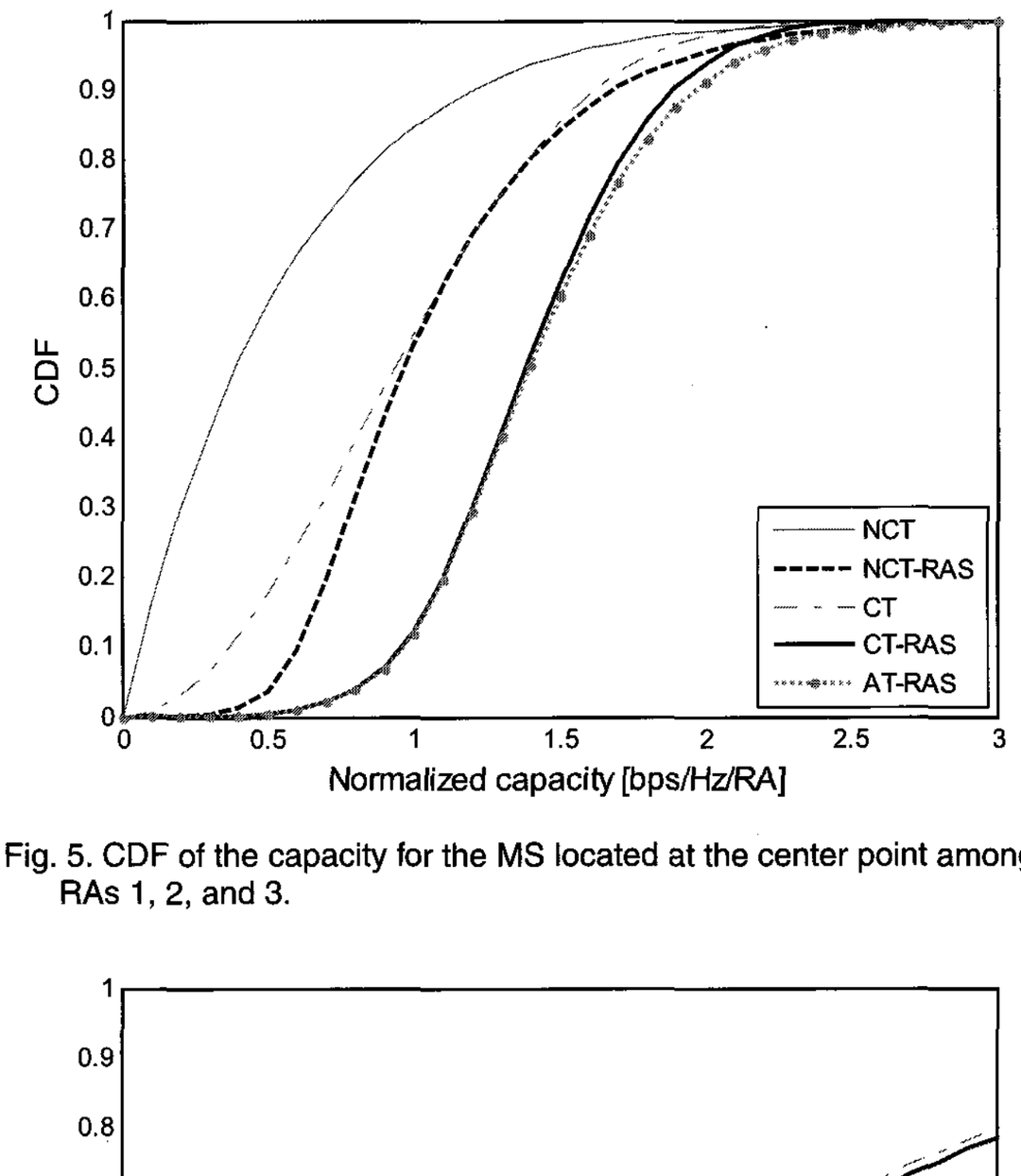


Fig. 5. CDF of the capacity for the MS located at the center point among RAs 1, 2, and 3.

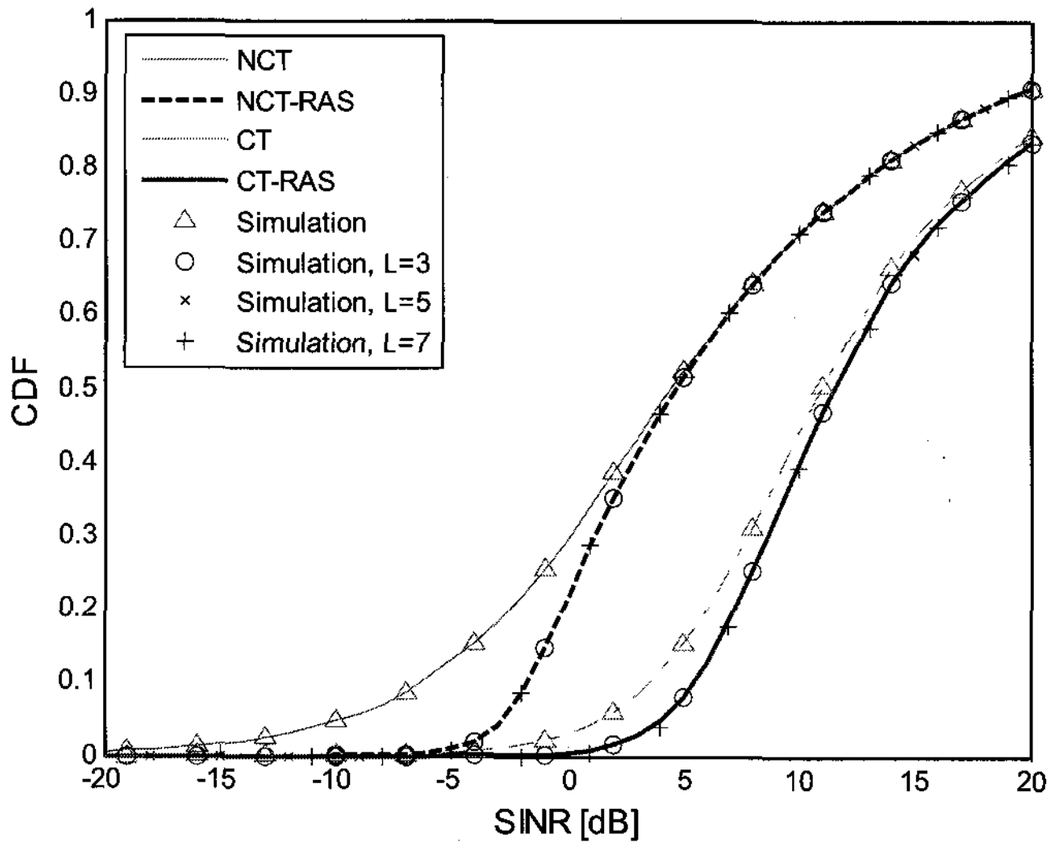


Fig. 4. CDF of the average SINR for the MS uniformly distributed over the geographic coverage of RA 1.

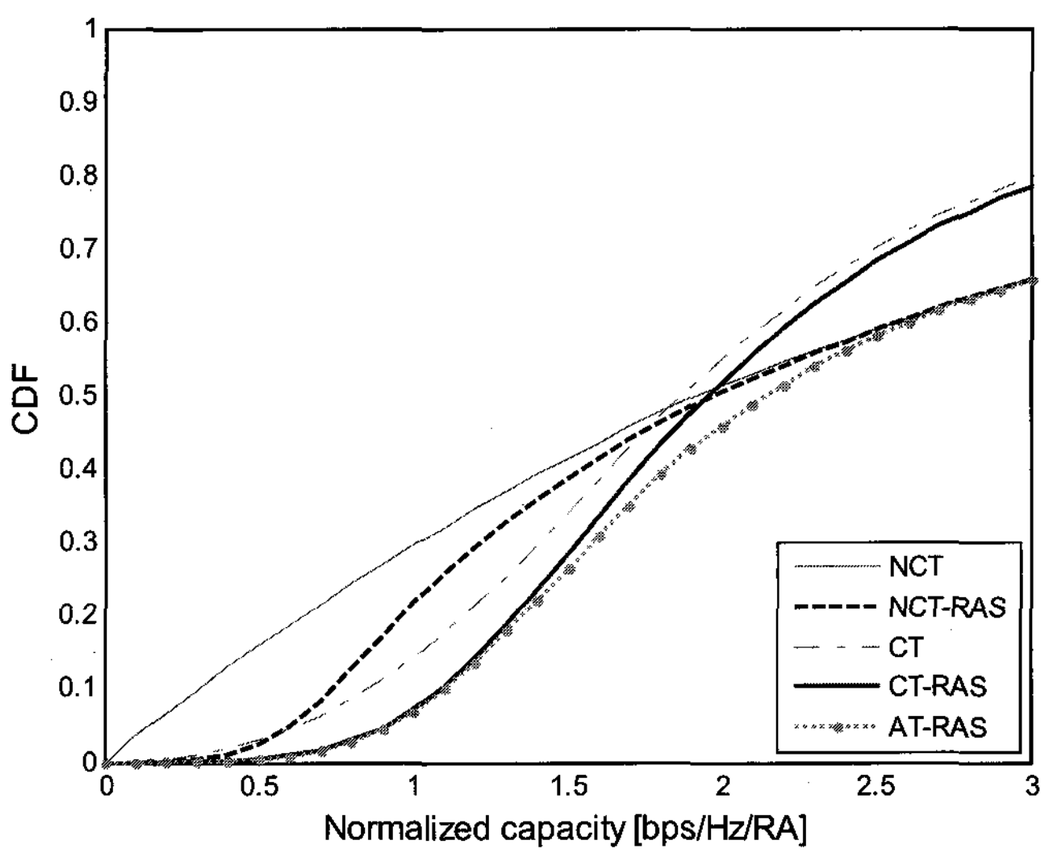


Fig. 6. CDF of the average capacity for the MS uniformly distributed over the geographic coverage of RA 1.

The derivation procedure and definitions of $\mu_1(\cdot)$, $\mu_2(\cdot)$, and $\mu_3(\cdot)$ are given in Appendix A. For the case of CT-RAS, the CDF of $\Gamma_{\text{CT}}(= 2\Gamma_{\max}^{(3,2)})$ is derived as

$$F_{\Gamma_{\text{CT}}}(\gamma) = F_{\Gamma_{\max}^{(3,2)}}\left(\frac{\gamma}{2}\right) = \begin{cases} 1-\nu_1(\frac{\gamma}{2}), & \text{for } \gamma \geq 2 \\ 1-\nu_1(\frac{\gamma}{2})-\nu_2(\frac{\gamma}{2}), & \text{for } 0 \leq \gamma < 2 \\ 0, & \text{otherwise} \end{cases} \tag{34}$$

for which the derivation procedure and definitions of $\nu_1(\cdot)$ and $\nu_2(\cdot)$ are given in Appendix B.

The CDFs for NCT, CT, NCT-RAS, and CT-RAS respectively given in (22), (23), (33), and (34) are plotted together in Fig. 3, for the MS located at the center point among RAs 1, 2, and 3 shown in Fig. 1. For this case, average values of the received power from three RAs are identical ($\lambda_1 = \lambda_2 = \lambda_3$). The 7-cell structure with 49 RAs and the parameters discussed in Section II are used for the numerical evaluation. We first observe the SINR performance gain of CT over NCT, which is approximately 9 dB without RA selection and 8 dB with RA selection at the median value. More importantly, we observe both CT and NCT performance enhances significantly, i.e., CDF curves shift to the right, when the RA selection is performed. Various performance quantities can be read from figures. For example, the probability of experiencing $-5$ dB SINR or below is approximately 60% for NCT, which decreases to about 3% for CT. When the RA selection is used, a further reduction of the probability occurs.

SINR distributions from the simulation are also shown in the figure. The simulated SINR values are obtained from repeated random generations of the signal from 49 RAs, with the average received power determined from the cell geometry. It is observed that all analytic curves are in good agreement with the simulation results. For the case of maximum SINR with RA selection, the multiple simulation results are obtained by using $L = 3$ (RAs 1, 2, and 3), $L = 5$ (RAs 1, 2, 3, 4, and 7 in Fig. 1), and $L = 7$ (all 7 RAs in Fig. 1). The results show that select-

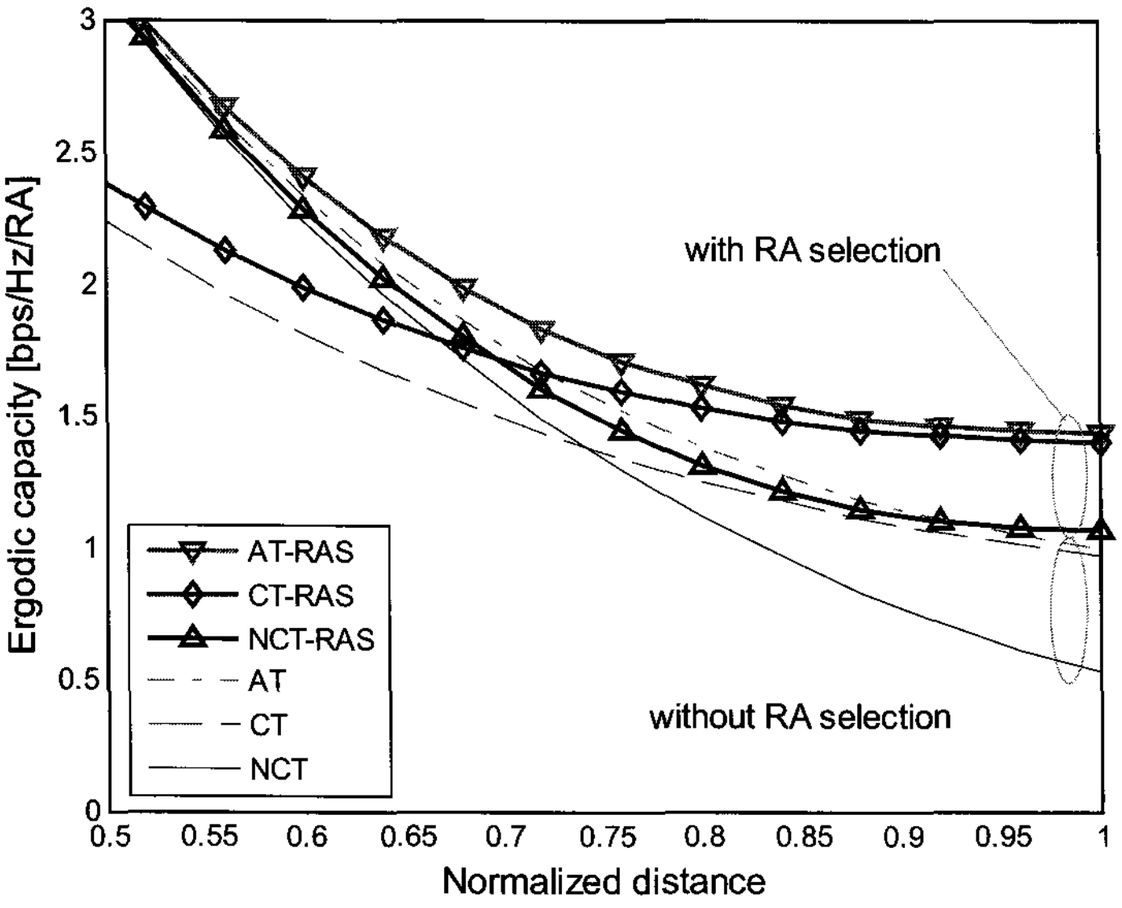


Fig. 7. Ergodic capacity for different transmission schemes at varying distances from the reference RA.

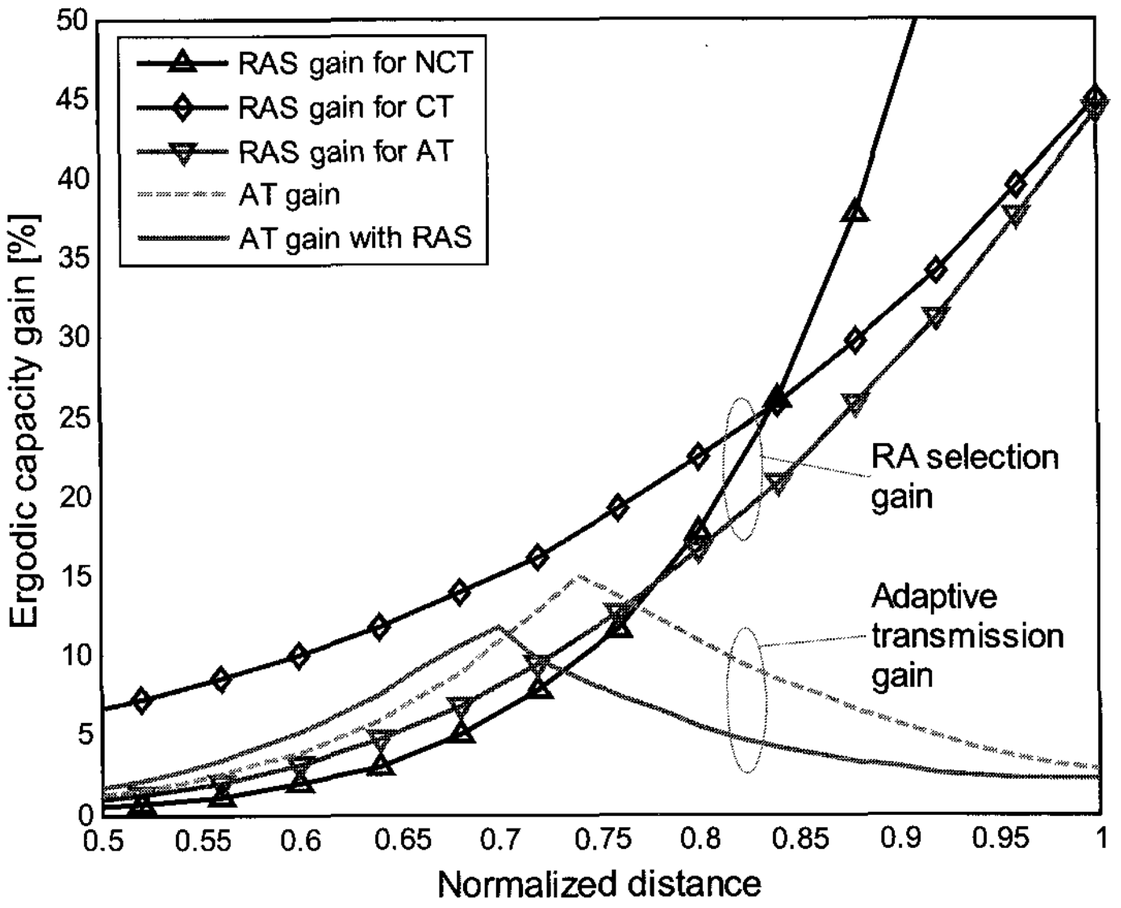


Fig. 8. Ergodic capacity gain among transmission schemes.

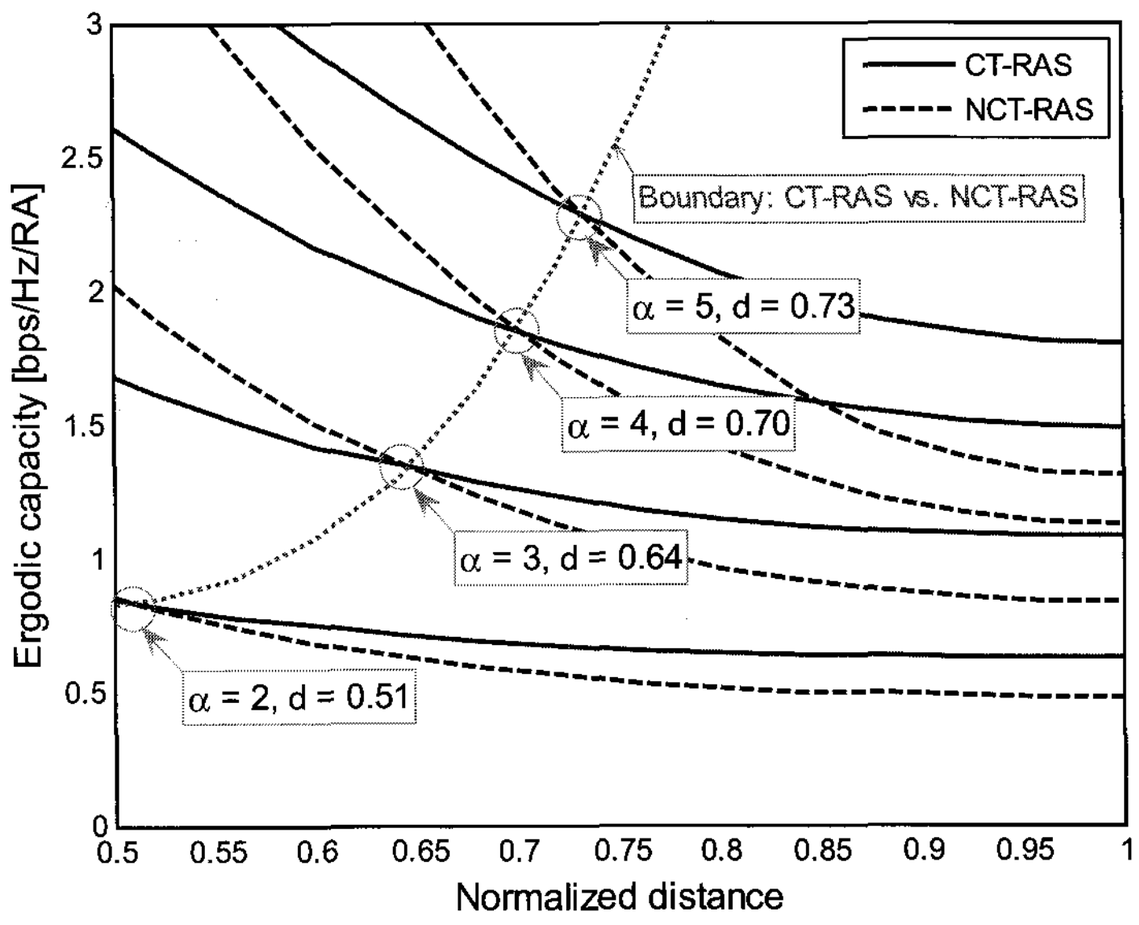


Fig. 9. Ergodic capacity of NCT and CT with RA selection for different pathloss exponent values.

ing RAs from more than 3 closest ones to the receiver produces virtually no gain in terms of the maximum SINR.

Fig. 4 shows the CDF for the MS uniformly located over the geographical coverage of RA 1, i.e., the MS is closest to RA 1 within the triangle connecting three RAs. The curves in the figure are obtained from the numerical integration of the CDF formulas, following the similar procedure as described in [32]. As expected, the figure indicates the gain from using RA selection is most significant in low SINR regions which corresponds to RA coverage boundaries. Simulation results for this case are also in good agreement with the analytic results.

### C. Capacity Distributions

The derived SINR distributions can be applied to obtain capacity distributions by the simple change of variable in CDF expressions. The CDFs of the normalized capacity for NCT and CT are respectively determined by

$$F_{\phi_{\text{NCT}}}(\eta) = F_{\gamma_{\text{NCT}}}(2^{\eta} - 1) \tag{35}$$

and

$$F_{\phi_{\text{CT}}}(\eta) = F_{\gamma_{\text{CT}}}(2^{2\eta} - 1). \tag{36}$$

The CDF of the normalized capacity for AT is obtained as

$$F_{\phi_{\text{AT}}}(\eta) = \int_0^{\eta} \int_0^{\eta} f_{\phi_{\text{NCT}},\phi_{\text{CT}}}(\eta_1, \eta_2) d\eta_1 d\eta_2 \tag{37}$$

where $f_{\phi_{\text{NCT}},\phi_{\text{CT}}}(\eta_1, \eta_2)$ is the joint pdf of $\phi_{\text{NCT}}$ and $\phi_{\text{CT}}$, which can be determined using the Jacobian transformation [39] of the joint pdf $f_{P_1,P_2,P_3}(p_1, p_2, p_3) = f_{P_1}(p_1) f_{P_2}(p_2) f_{P_3}(p_3)$. The corresponding CDFs of the normalized capacity $\Phi_{\text{NCT}}$, $\Phi_{\text{CT}}$, and $\Phi_{\text{AT}}$ with RA selection can be similarly obtained.

In Fig. 5, the CDFs of the normalized capacity are plotted for the MS located in the center point among RAs 1, 2, and 3 using the derivation result, which quantify the gain from using cooperative transmission as well as the gain from performing the RA selection. At the median value, the CT gain is approximately 0.42 bps/Hz/RA for fixed RAs, and 0.55 bps/Hz/RA for the RA selection. Also, the gain produced by the RA selection is 0.58 bps/Hz/RA for NCT and 0.46 bps/Hz/RA for CT. Fig. 6 shows the CDFs of the normalized capacity for the MS uniformly located over the coverage area of RA 1, representing the cell-average capacity distributions. In this figure, crossing between the CDFs for NCT and CT can be found, since NCT outperforms CT in terms of the normalized capacity at locations with dominating received signal power from a single RA. However, the capacity obtained from using the RA selection always exceeds the capacity for fixed RAs. The highest spectral efficiency is achieved by AT-RAS, shown as the rightmost curves in Figs. 5 and 6.

## V. PERFORMANCE EVALUATION

Ergodic capacity for each transmission mode is evaluated and compared in Fig. 7, where the plotted curves are obtained from

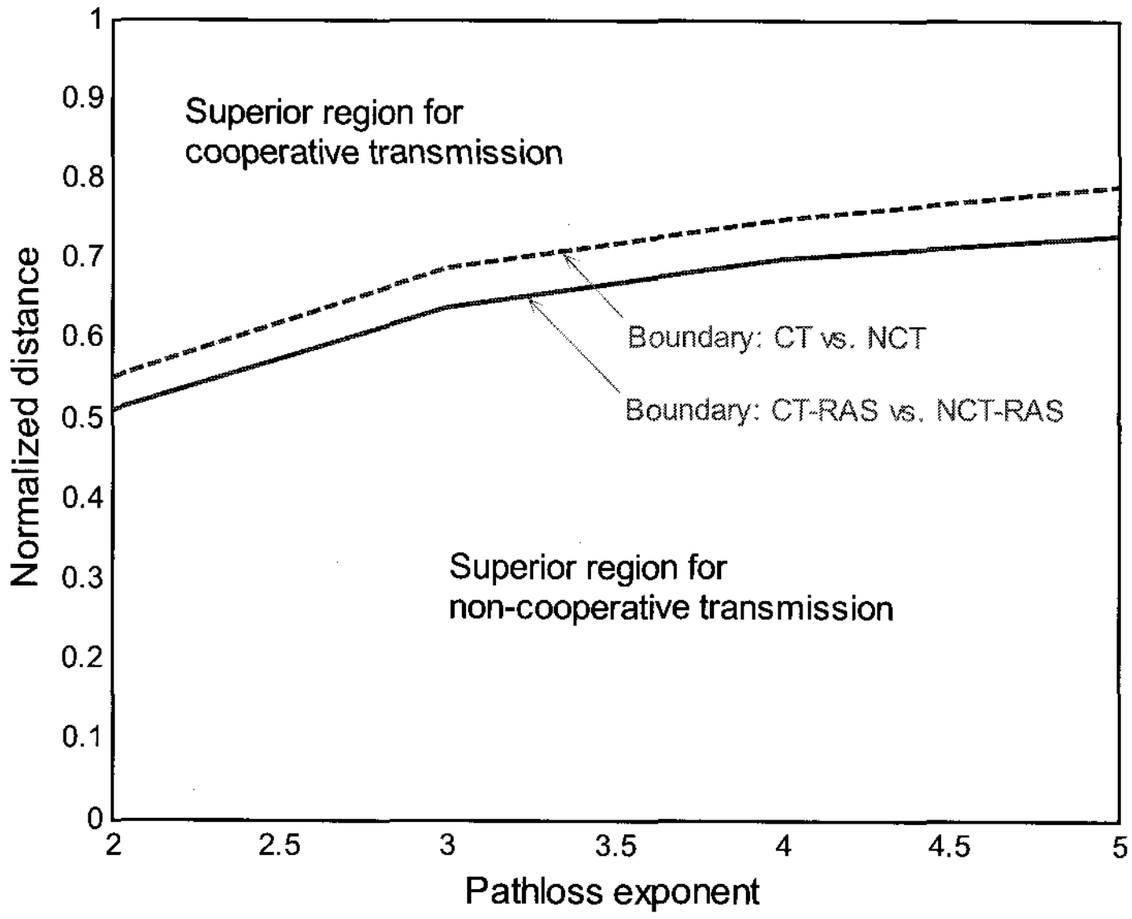


Fig. 10. Superior regions for NCT and CT maximizing the capacity with and without RA selection.

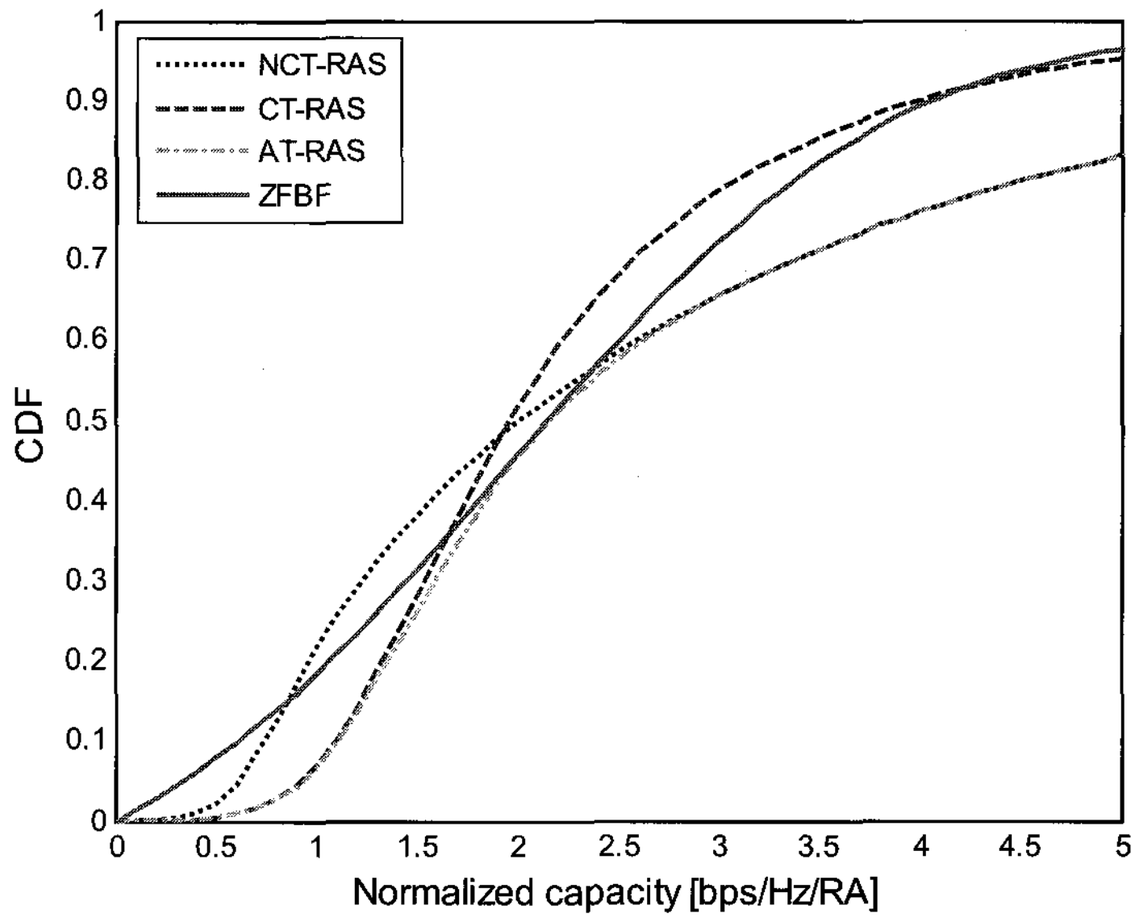


Fig. 11. CDF of the average capacity: Zero-forcing beamforming vs. transmission with RA selection.

the numerical integration using the corresponding pdfs. For example, the ergodic capacity for NCT is computed as

$$\bar{\phi}_{\text{NCT}} \triangleq \mathbb{E}[\phi_{\text{NCT}}] = \int_0^\infty \eta f_{\phi_{\text{NCT}}}(\eta) d\eta \tag{38}$$

using pdf $f_{\phi_{\text{NCT}}}(\eta)$ at a given location of the MS. Ergodic capacity values for the other transmission modes, i.e., $\bar{\phi}_{\text{CT}}$, $\bar{\phi}_{\text{AT}}$, $\bar{\Phi}_{\text{NCT}}$, $\bar{\Phi}_{\text{CT}}$, and $\bar{\Phi}_{\text{AT}}$ can be similarly determined.

As can be observed in the figure, the ergodic capacity values tend to decrease in general as the MS moves away from RA 1, due to the decreasing SINR. The three transmission modes with the RA selection, NCT-RAS, CT-RAS, and AT-RAS drawn in solid lines exhibit significantly improved capacity values over the transmission modes without RA selection, and the gain becomes more substantial as the MS approaches to normalized distance 1. It can be also verified from the figure that the crossover boundary at which NCT and CT have the identical capacity performance corresponds to normalized distance 0.74 without the RA selection and 0.69 with the RA selection, implying CT is desired for the capacity maximization for a wider geographical range when RAs are selected.

The amounts of capacity gain among different cooperation strategies are presented in Fig. 8. The gain achieved by using the RA selection is determined by computing $(\bar{\Phi}_{\text{NCT}} - \bar{\phi}_{\text{NCT}})/\bar{\phi}_{\text{NCT}}$, $(\bar{\Phi}_{\text{CT}} - \bar{\phi}_{\text{CT}})/\bar{\phi}_{\text{CT}}$, and $(\bar{\Phi}_{\text{AT}} - \bar{\phi}_{\text{AT}})/\bar{\phi}_{\text{AT}}$ for NCT, CT, and AT modes, respectively. Also shown in the figure are the amounts of capacity gain obtained by using AT, which are computed as

$$\frac{\bar{\Phi}_{\text{AT}} - \max(\bar{\Phi}_{\text{NCT}}, \bar{\Phi}_{\text{CT}})}{\max(\bar{\Phi}_{\text{NCT}}, \bar{\Phi}_{\text{CT}})} \quad \text{and} \quad \frac{\bar{\phi}_{\text{AT}} - \max(\bar{\phi}_{\text{NCT}}, \bar{\phi}_{\text{CT}})}{\max(\bar{\phi}_{\text{NCT}}, \bar{\phi}_{\text{CT}})}$$

for modes with and without the RA selection, respectively.

The ergodic capacities for CT-RAS and NCT-RAS are compared in Fig. 9 for different pathloss exponent values $\alpha = 2, 3, 4$, and 5. We observe the increase in capacity as $\alpha$ becomes larger, implying the receiver SINR improves as the propagation pathloss increases, i.e., the attenuation of interference is more dominant in determining the SINR than the attenuation of the desired signal. It is also observed from the figure that as the pathloss exponent increases, the amount of capacity gain near normalized distance 1 is more substantial for CT than NCT, i.e., the cooperation becomes more advantageous. On the other hand, the crossover boundary between CT and NCT becomes closer to normalized distance 1 as $\alpha$ increases, to result in a reduced range for cooperation. The preferred region of performing either CT or NCT for capacity maximization is indicated for various values of $\alpha$ in Fig. 10, which shows the region for cooperation becomes larger when RA selection is applied.

The presented results can also be compared with the performance of multiuser multiple-input multiple-output transmission [40]. A well-known transmission method using distributed antennas to support multiple MSs simultaneously is zero-forcing beamforming (ZFBF) proposed in [1]. We evaluate the CDF of the normalized capacity for the ZFBF method which is plotted in Fig. 11 for comparison. For the performance evaluation of ZFBF, 3 MSs are uniformly generated over the geographic coverage of RAs 1, 2, and 3 (within the triangle connecting the RAs) and the capacity per RA is computed using the procedure described in [1]. It is observed in the figure that outperforming transmission schemes differ depending on the range of capacity values. When compared to NCT-RAS and CT-RAS, ZFBF exhibits improved performance of mid-range capacity values (e.g., 0.86 to 2.37 bps/Hz/RA when compared to NCT-RAS). For low and high extreme capacity values, transmission with RA selection performs better, suggesting the RA selection can be the preferred method of operation for certain geographic locations including RA coverage boundaries. It can be also observed AT-RAS outperform ZFBF for nearly entire range of the capacity values. We have limited the number of participating RAs to three for all transmission schemes in this experiment, for comparable system operational complexity. As the number of participating RAs increase, additional capacity gain may be attained using ZFBF.

## VI. CONCLUSIONS

Cooperative transmission is an efficient means to improve the received signal quality, especially near the antenna coverage boundaries. We demonstrated that such an advantage of cooperative transmission in distributed MISO systems can be further enhanced when transmission antennas are adaptively selected based on the channel condition, by presenting various statistics indicating the gain in terms of the SINR and the normalized capacity. For the achievable maximum SINR using antenna selection, we presented a general expression as well as closed-form formulas for the distribution.

## APPENDICES

### I. DERIVATION FOR THE CDF OF $\Gamma_{\max}^{(3,1)}$

Using index sets $\mathcal{D}_n = \{i\}$ and $\mathcal{I}_n = \{j,k\}$, the integration inside the square brackets in (32) can be written as

$$\begin{aligned}\int_{p_{(2)}}^{v\gamma} f_{U_n,V_n}(u,v)du &= \int_{p_{(2)}}^{v\gamma} f_{P_i,P_j+P_k+\sigma_I^2}(u,v)du \\ &= \int_{p_{(2)}}^{v\gamma} f_{P_i,P_j+P_k}(u,v-\sigma_I^2)du.\end{aligned}$$

From the convolution integral in (27) with the first condition given by (28), we obtain

$$\int_{p_{(2)}}^{v\gamma} f_{U_n,V_n}(u,v)du = \int_{p_{(2)}}^{v\gamma} f_{P_i}(p_i)\left(\int_0^{v-\sigma_I^2} f_{P_j}(p_j)f_{P_k}(p_k)dp_j\right)dp_i$$

where $p_i = u$ and $p_k = v - p_j - \sigma_I^2$. The integration ranges for $p_i$ and $p_j$ are illustrated in Fig. 12(a). Using the second condition in (29), $p_{(2)}$ can be determined as $p_{(2)} = p_j$ for $p_j \geq (v-\sigma_I^2)/2$, and $p_{(2)} = p_k$ otherwise. Thus, the convolution equation above is further determined as shown in Fig. 12(b) as

$$\begin{aligned}&\int_{p_{(2)}}^{v\gamma} f_{U_n,V_n}(u,v)du \\ &= \int_{p_k}^{v\gamma} f_{P_i}(p_i)\left(\int_0^{\frac{v-\sigma_I^2}{2}} f_{P_j}(p_j)f_{P_k}(p_k)dp_j\right)dp_i \\ &\quad + \int_{p_j}^{v\gamma} f_{P_i}(p_i)\left(\int_{\frac{v-\sigma_I^2}{2}}^{v-\sigma_I^2} f_{P_j}(p_j)f_{P_k}(p_k)dp_j\right)dp_i.\end{aligned}$$

Applying this result into the generalized maximum CDF in (32), we obtain

$$F_{\Gamma_{\max}^{(3,1)}}(\gamma) = \int_{\sigma_I^2}^{\infty} \Omega(c,d;v,\gamma,\sigma_I^2)dv$$

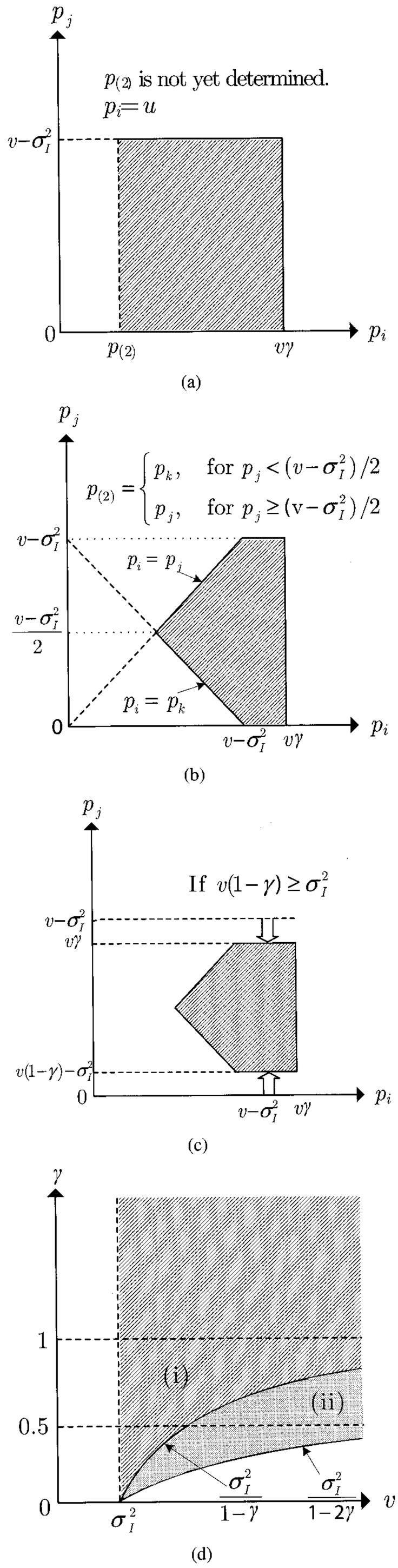


Fig. 12. Integration ranges for the CDF of $\Gamma_{\max}^{(3,1)}$: (a) The first condition, (b) the second condition, (c) the third condition, and (d) the relation between $\gamma$ and $v$.

where

$$\Omega(c,d;v,\gamma,\sigma_I^2) \triangleq \sum_{\substack{i=1,\\ j=(i+1)_3,\\ k=(i+2)_3}}^{3} \left\{ \int_c^{\frac{v-\sigma_I^2}{2}} f_{P_j}(p_j) f_{P_k}(p_k) \left( \int_{p_k}^{v\gamma} f_{P_i}(p_i) dp_i \right) dp_j + \int_{\frac{v-\sigma_I^2}{2}}^{d} f_{P_j}(p_j) f_{P_k}(p_k) \left( \int_{p_j}^{v\gamma} f_{P_i}(p_i) dp_i \right) dp_j \right\}$$

and the notation $(\cdot)_3$ represents the modulo-3 operation. The third condition in (31) provides criteria to determine variables $c$ and $d$ as follows:

**Case (i):** When $v(1-\gamma) - \sigma_I^2 < 0$ (represented by the shaded region (i) in Fig. 12(d)), the third condition does not set additional constraints and the integration range is as shown in Fig. 12(b), for which case $[c,d] = [0, v-\sigma_I^2] \triangleq [c_1, d_1]$.

**Case (ii):** When $0 \le v(1-\gamma) - \sigma_I^2 \le v\gamma$ (represented by the shaded region (ii) in Fig. 12(d)), the third condition $p_{(2)} \le v\gamma$ requires

$$v(1-\gamma) - \sigma_I^2 \le p_j$$

for the case of $p_{(2)} = p_k = v - p_j - \sigma_I^2$, and

$$p_j \le v\gamma$$

for the case of $p_{(2)} = p_j$. The corresponding range of integration is shown in Fig. 12(c), and we have $[c,d] = [v(1-\gamma)-\sigma_I^2, v\gamma] \triangleq [c_2, d_2]$.

Therefore, the CDF of the maximum SINR for $F_{\Gamma_m^{(3,1)}}(\gamma)$ is determined for different ranges of $\gamma$ shown in Fig. 12(d) as

$$F_{\Gamma_{\max}^{(3,1)}}(\gamma) = \begin{cases} \int_{\sigma_I^2}^{\infty} \Omega(c_1,d_1;v,\gamma,\sigma_I^2)dv, & \text{for } \gamma \ge 1 \\ \int_{\sigma_I^2}^{\frac{\sigma_I^2}{1-\gamma}} \Omega(c_1,d_1;v,\gamma,\sigma_I^2)dv + \int_{\frac{\sigma_I^2}{1-\gamma}}^{\infty} \Omega(c_2,d_2;v,\gamma,\sigma_I^2)dv, & \text{for } \frac{1}{2} \le \gamma < 1 \\ \int_{\sigma_I^2}^{\frac{\sigma_I^2}{1-\gamma}} \Omega(c_1,d_1;v,\gamma,\sigma_I^2)dv + \int_{\frac{\sigma_I^2}{1-\gamma}}^{\frac{\sigma_I^2}{1-2\gamma}} \Omega(c_2,d_2;v,\gamma,\sigma_I^2)dv, & \text{for } 0 \le \gamma < \frac{1}{2} \\ 0, & \text{otherwise.} \end{cases} \quad (39)$$

By evaluating the integral in (39), a closed-form formula for $F_{\Gamma_m^{(3,1)}}(\gamma)$ is obtained as

$$F_{\Gamma_{\max}^{(3,1)}}(\gamma) = \begin{cases} 1-\mu_1(\gamma), & \text{for } \gamma \ge 1 \\ 1-\mu_1(\gamma)-\mu_2(\gamma), & \text{for } \frac{1}{2} \le \gamma < 1 \\ 1-\mu_1(\gamma)-\mu_2(\gamma)-\mu_3(\gamma), & \text{for } 0 \le \gamma < \frac{1}{2} \\ 0, & \text{otherwise} \end{cases}$$

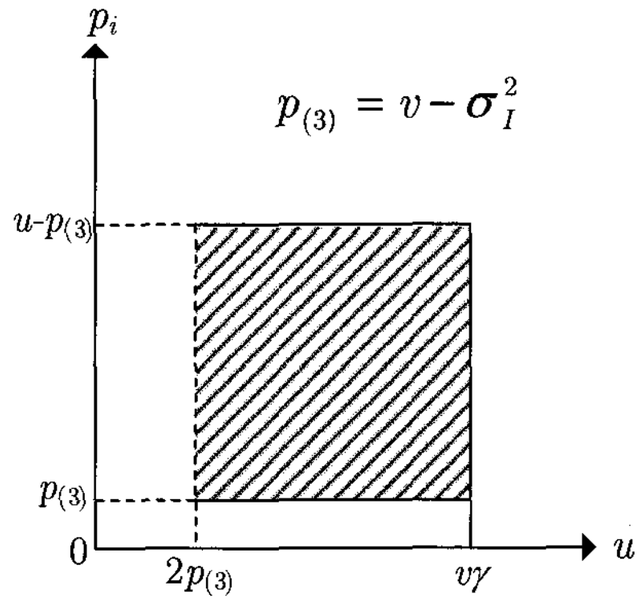


Fig. 13. Integration ranges for the CDF of $\Gamma_{\max}^{(3,2)}$: (a) The first and second condition and (b) the relation between $\gamma$ and $v$.

where $\mu_1(\cdot)$, $\mu_2(\cdot)$, and $\mu_3(\cdot)$ are given in (41)–(43), respectively.

## II. DERIVATION FOR THE CDF OF $\Gamma_{\max}^{(3,2)}$

With index sets $\mathcal{D}_n = \{i,j\}$ and $\mathcal{I}_n = \{k\}$, the integration inside the square brackets in (32) becomes

$$\int_{2p_{(3)}}^{v\gamma} f_{U_n,V_n}(u,v)du = \int_{2p_{(3)}}^{v\gamma} f_{P_i+P_j,P_k}(u, v-\sigma_I^2)du.$$

By applying the convolution integral in (27) with the first and second conditions given by (28) and (29), we have

$$\int_{2p_{(3)}}^{v\gamma} f_{U_n,V_n}(u,v)du = \int_{2p_{(3)}}^{v\gamma} \left( \int_{p_{(3)}}^{u-p_{(3)}} f_{P_i}(p_i) f_{P_j}(p_j) dp_i \right) f_{P_k}(p_k)du = \int_{2p_k}^{v\gamma} \left( \int_{p_k}^{u-p_k} f_{P_i}(p_i) f_{P_j}(p_j) dp_i \right) f_{P_k}(p_k)du \quad (40)$$

where $p_j = u - p_i$ and $p_k = v - \sigma_I^2$ with the integration range as shown in Fig. 13(a). The third condition given by (31) is equivalent to $v\gamma \ge 2(v-\sigma_I^2)$, which always holds when $\gamma \ge 2$. If $\gamma < 2$, an additional constraint

$$v \le 2\sigma_I^2/(2-\gamma)$$

$$\mu_1(\gamma) = \sum_{\substack{i=1, j=(i+1)_3, \\ k=(i+2)_3}}^{3} \frac{e^{-\frac{\gamma\sigma_I^2}{\lambda_i}}\lambda_i^2}{(\lambda_i+\gamma\lambda_j)(\lambda_i+\gamma\lambda_k)} \tag{41}$$

$$\mu_2(\gamma) = \sum_{\substack{i=1, j=(i+1)_3, \\ k=(i+2)_3}}^{3} \frac{-e^{\frac{\gamma(\lambda_i+\lambda_j)\sigma_I^2}{(\gamma-1)\lambda_i\lambda_j}}(\gamma-1)^2(\gamma+1)\lambda_i^2\lambda_j^2}{((1-\gamma)\lambda_i\lambda_j+\gamma(\lambda_i+\lambda_j)\lambda_k)(\gamma\lambda_i+\lambda_j)(\lambda_i+\gamma\lambda_j)} \tag{42}$$

$$\mu_3(\gamma) = \prod_{\substack{i=1, j=(i+1)_3, \\ k=(i+2)_3}}^{3} \frac{e^{\frac{\gamma\sigma_I^2}{(2\gamma-1)\lambda_i}}(1-2\gamma)^2(\gamma+1)\lambda_i^2}{(1-\gamma)\lambda_j\lambda_k+\gamma\lambda_i(\lambda_j+\lambda_k)} \tag{43}$$

$$\nu_1(\gamma) = \begin{cases} \dfrac{3e^{-\frac{\gamma\sigma_I^2}{\lambda}}((2\gamma-1)\lambda+\gamma(\gamma+1)\sigma_I^2)}{(\gamma+1)^2\lambda}, & \text{if } \lambda_i=\lambda_j=\lambda_k \\ \displaystyle\sum_{\substack{i=1, j=(i+1)_3, \\ k=(i+2)_3}}^{3} \frac{e^{-\frac{\gamma\sigma_I^2}{\lambda_i}}\lambda_i^2(-\lambda_i\lambda_j+2\lambda_k\lambda_j-\lambda_i\lambda_k)}{(\lambda_i-\lambda_j)(\lambda_i-\lambda_k)(-\lambda_i\lambda_j+(1-\gamma)\lambda_k\lambda_j-\lambda_i\lambda_k)}, & \text{if } \lambda_1\neq\lambda_2\neq\lambda_3 \\ \dfrac{e^{-\frac{\gamma\sigma_I^2}{\lambda}}\left(-\lambda\left(\lambda^2+(2\gamma-1)\lambda'\lambda+2\lambda'^2\right)-\gamma(\lambda-\lambda')(\lambda+\gamma\lambda')\sigma_I^2\right)}{(\lambda-\lambda')(\lambda+\gamma\lambda')^2} & \\ \qquad +\dfrac{2e^{-\frac{\gamma\sigma_I^2}{\lambda'}}\lambda'^2}{(\lambda'-\lambda)((\gamma-1)\lambda+2\lambda')}, & \text{if } \lambda_i=\lambda_j=\lambda\neq\lambda_k, \forall i,j,k\in\{1,2,3\} \end{cases} \tag{44}$$

$$\nu_2(\gamma) = \prod_{\substack{i=1, j=(i+1)_3, \\ k=(i+2)_3}}^{3} \frac{e^{\frac{\gamma\sigma_I^2}{(\gamma-2)\lambda_i}}(\gamma-2)^2(\gamma+1)\lambda_i^2}{(\gamma-1)\lambda_i\lambda_j+(\lambda_i+\lambda_j)\lambda_k} \tag{45}$$

is required, resulting in the range for $v$ as $[\sigma_I^2, 2\sigma_I^2/(2-\gamma)]$. The relation between $\gamma$ and $v$ for this case is illustrated in Fig. 13(b). Combining (40) into (32), we obtain

$$F_{\Gamma_{\max}^{(3,2)}}(\gamma) = \begin{cases} \displaystyle\int_{\sigma_I^2}^{\infty} \Psi(v,\gamma,\sigma_I^2)dv, & \text{for } \gamma\geq 2 \\ \displaystyle\int_{\sigma_I^2}^{\frac{2\sigma_I^2}{(2-\gamma)}} \Psi(v,\gamma,\sigma_I^2)dv, & \text{for } 0\leq\gamma<2 \\ 0, & \text{otherwise} \end{cases}$$

where

$$\Psi(v,\gamma,\sigma_I^2) \triangleq \sum_{\substack{i=1, \\ j=(i+1)_3, \\ k=(i+2)_3}}^{3} \int_{2p_k}^{v\gamma} \left( \int_{p_k}^{u-p_k} f_{P_i}(p_i) f_{P_j}(p_j) dp_i \right) f_{P_k}(p_k) du$$

and the resulting closed-form expression is

$$F_{\Gamma_{\max}^{(3,2)}}(\gamma) = \begin{cases} 1-\nu_1(\gamma), & \text{for } \gamma\geq 2 \\ 1-\nu_1(\gamma)-\nu_2(\gamma), & \text{for } 0\leq\gamma<2 \\ 0, & \text{otherwise} \end{cases}$$

for which $\nu_1(\cdot)$ and $\nu_2(\cdot)$ are respectively given in (44) and (45).

## REFERENCES


[1] M. K. Karakayali, G. J. Foschini, and R. A. Valenzuela, "Network coordination for spectrally efficient communications in cellular systems," *IEEE Wireless Commun.*, vol. 13, no. 4, pp. 56–61, Aug. 2006.

[2] J. N. Laneman, D. N. C. Tse, and G. W. Wornell, "Cooperative diversity in wireless networks: Efficient protocols and outage behavior," *IEEE Trans. Inf. Theory*, vol. 50, no. 12, pp. 3062–3080, Dec. 2004.

[3] H. Zhang and H. Dai, "Cochannel interference mitigation and cooperative processing in downlink multiuser MIMO networks," *Eur. J. Wireless Commun. Netw.*, no. 2, pp. 222–235, 2004.

[4] B. L. Ng, J. S. Evans, S. V. Hanly, and D. Aktas, "Transmit beamforming with cooperative base stations," in *Proc. ISIT 2005*, Sept. 2005, pp. 1431–1435.

[5] L. Dai, S. D. Zhou, and Y. Yao, "Capacity analysis in CDMA distributed antenna systems," *IEEE Trans. Wireless Commun.*, vol. 4, no. 6, pp. 2613–2620, Nov. 2005.

[6] P. W. Baier, M. Meurer, T. Weber, and H. Troeger, "Joint transmission (JT), an alternative rationale for the downlink of time division CDMA using multi-element transmit antennas," in *Proc. ISSSTA 2000*, Sept. 2000, pp. 1–5.

[7] S.-L. Su, J.-Y. Chen, and J.-H. Huang, "Performance analysis of soft handoff in CDMA cellular networks," *IEEE J. Sel. Areas Commun.*, vol. 14, no. 9, pp. 1762–1769, Dec. 1996.

[8] C. Mihailescu, X. Lagrange, and P. Godlewski, "Soft handover analysis in downlink UMTS WCDMA systems," in *Proc. IEEE MOMUC'99*, Nov. 1999.

[9] Y. Chen and L. Cuthbert, "Optimum size of soft handover zone in power-controlled UMTS downlink systems," *Electron. Lett.*, vol. 38, no. 2, pp. 89–90, Jan. 2002.

[10] J. Wei, H. Zhao, and S. Wang, "Cooperative transmission in the wireless

sensors network: Realization and analysis," in *Proc. WiCOM 2006*, Sept. 2006, pp. 1–4.
[11] A. A. M. Saleh, A. J. Rustako, and R. S. Roman, "Distributed antennas for indoor radio communications," *IEEE Trans. Commun.*, vol. 35, no. 12, pp. 1245–1251, Dec. 1987.
[12] W. Roh and A. Paulraj, "Outage performance of the distributed antenna systems in a composite fading channel," in *Proc. IEEE VTC 2002-fall*, Sept. 2002. pp. 1520–1524.
[13] L. Xiao, L. Dai, H. Zhuang, S. Zhou, and Y. Yao, "Information-theoretic capacity analysis in MIMO distributed antenna systems," in *Proc. IEEE VTC 2003-spring*, Apr. 2003, pp. 779–782.
[14] R. E. Schuh and M. Sommer, "W-CDMA coverage and capacity analysis for active and passive distributed antenna systems," in *Proc. IEEE VTC 2002-spring*, May 2002. pp. 434–438.
[15] R. Hasegawa, M. Shirakabe, R. Esmailzadeh, and M. Nakagawa, "Downlink performance of a CDMA system with distributed base station," in *Proc. IEEE VTC 2003-fall.*, Oct. 2003, pp. 882–886.
[16] H. Zhuang, L. Dai, L. Xiao, and Y. Yao, "Spectral efficiency of distributed antenna systems with random antenna layout," *Electron. Lett.*, vol. 39, no. 6, pp. 495–496, Mar. 2003.
[17] W. Choi and J. G. Andrews, "Downlink performance and capacity of distributed antenna systems in a multicell environment," *IEEE Trans. Wireless Commun.*, vol. 6, no. 1, pp. 69–73, Jan. 2007.
[18] S. Zhou, M. Zhao, X. Xu, J. Wang, and Y. Yao, "Distributed wireless communication system: A new architecture for future public wireless access," *IEEE Commun. Mag.*, vol. 41, no. 3, pp. 108–113, Mar. 2003.
[19] A. Sendonaris, E. Erkip, and B. Aazhang, "User cooperation diversity part I and part II," *IEEE Trans. Commun.*, vol. 51, no. 11, pp. 1927–1948, Nov. 2003.
[20] A. Nosratinia, T. Hunter, and A. Hedayat, "Cooperative communication in wireless networks," *IEEE Commun. Mag.*, vol. 42, no. 10, pp. 74–80, Oct. 2004.
[21] J. N. Laneman and G. W. Wornell, "Distributed space-time coded protocols for exploiting cooperative diversity in wireless networks," *IEEE Trans. Inf. Theory*, vol. 49, no. 10, pp. 2415–2425, Oct. 2003.
[22] E. Song, J. Park, J. Kim, S. Hwang, and W. Sung, "Performance of cooperative transmission schemes using distributed antennas," in *Proc. IEEE CCNC 2008*, Jan. 2008.
[23] J. Park, E. Song, J. Kim, S. Hwang, and W. Sung, "Capacity and outage performance of regional signal combining using distributed antennas," in *Proc. IEEE APCC 2007*, Oct. 2007, pp. 261–264.
[24] S. Alamouti, "A simple transmit diversity technique for wireless communications," *IEEE J. Sel. Areas Commun.*, vol. 16, no. 8, pp. 1451–1458, Oct. 1998.
[25] T. Xiaofeng, H. Harald, Y. Zhizhuan, Q. Haiyan, and Z. Ping, "Closed loop space-time block code," in *Proc. IEEE VTC 2002-fall*, vol. 2, Oct. 2001, pp. 1093–1096.
[26] D. J. Love and R. W. Heath, "Equal gain transmission in multiple-input multiple-output wireless systems," *IEEE Trans. Commun.*, vol. 51, no. 7, pp. 1102–1110, July 2003.
[27] T. K. Y. Lo, "Maximum ratio transmission," *IEEE Trans. Commun.*, vol. 47, no. 10, pp. 1458–1461, Oct. 1999.
[28] L. C. Wang and C. T. Lea, "Macrodiversity cochannel interference analysis," *Electron. Lett.*, vol. 31, no.8, pp. 614–616, Apr. 1995.
[29] Y.-D. Yao and A. U. H. Sheikh, "Investigation into cochannel interference in microcellular mobile radio systems," *IEEE Trans. Veh. Technol.*, vol. 41, no. 2, pp. 114–123, May 1992.
[30] J. Zhang and V. A. Aalo, "Effect of macrodiversity on average-error probabilities in a Rician fading channel with correlated lognormal shadowing," *IEEE Trans. Commun.*, vol. 49, no. 1, pp. 14–18, Jan. 2001.
[31] T. Piboongungon and V. A. Aalo, "Outage probability of L-branch selection combining in correlated lognormal fading channels," *Electron. Lett.*, vol. 40, no. 14, pp. 886–888, July 2004.
[32] S. Mukherjee and D. Avidor, "Effect of microdiversity and correlated macrodiversity on outages in a cellular system," *IEEE Trans. Wireless Commun.*, vol. 2, no. 1, pp. 50–58, Jan. 2003.
[33] 3GPP TR 25.892, *Feasibility Study for Orthogonal Frequency Division Multiplexing for UTRAN Enhancement*. V2.0.0, June 2004.
[34] H. T. Cheng, H. Mheidat, M. Uysal, and T. M. Lok, "Distributed space-time block coding with imperfect channel estimation," in *Proc. ICC 2005*, May 2005, pp. 583–587.
[35] P. Viswanath, D. N. C. Tse, and R. Laroia, "Opportunistic beamforming using dumb antennas," *IEEE Trans. Inf. Theory*, vol. 48, no. 6, pp. 1277–1294, June 2002.
[36] J. G. Proakis, *Digital Communications*, 4th. ed. New York: McGraw-Hill, 2001.
[37] V. K. Rohatgi, *An Introduction to Probability Theory and Mathematical Statistics*. New York: Wiley, 1976.
[38] H. A. David, *Ordered Statistics*. New York: Wiley, 2003.
[39] A. Papoulis, *Probability, Random Variables, and Stochastic Processes*, 4th ed. New York: McGraw-Hill, 2002.
[40] Q. H. Spencer, C. B. Peel, A. L. Swindlehurst, and M. Haardt, "An introduction to the multi-user MIMO downlink," *IEEE Commun. Mag.*, vol. 39, no. 10, pp. 60–67, Oct. 2004.

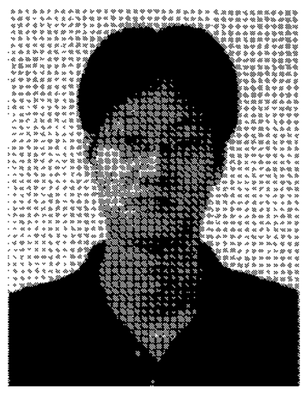

**Jonghyun Park** was born in Seoul, Korea, April 10, 1979. He received the B.S. and M.S. degrees in Electronic Engineering from Sogang University, Seoul, Korea in 2004 and 2006, respectively. He is currently pursuing his Ph.D. degree in Electronic Engineering at Sogang University. His research interests include signal processing for high-speed digital communications, distributed wireless communication systems, space-time signal processing, and cross-layer design for multi-user MIMO.

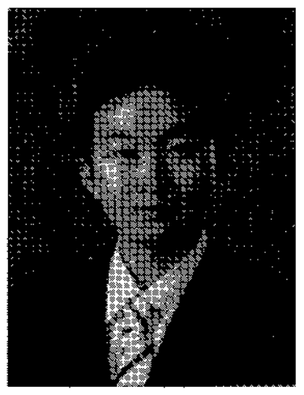

**Jaewon Kim** was born in Seoul, Korea, November 10, 1981. He received the B.S. degree in Electronic Engineering from Sogang University, Seoul, Korea in 2006. He is pursuing his M.S. degree at Sogang University. His research interests include statistic analysis, communication signal processing, space-time coding, and multi-user MIMO systems. He received the Best Paper Award from the 18th Joint Conference on Communications and Information held in Jeju, Korea in April 2008.

**Wonjin Sung** received his B.S. degree from Seoul National University, Korea in 1990, and the M.S. and Ph.D. degrees in Electrical Engineering from University of Michigan, Ann Arbor, MI, in 1992 and 1995, respectively. From January 1996 through August 2000, He worked at Hughes Network Systems, Germantown, MD, USA, where he participated in development projects for cellular and satellite systems including base station modems for the IS-136 North American TDMA, multi-mode terminals for medium orbit satellites, and the Inmarsat air interface design. Since September 2000, he has been with the Department of Electronic Engineering at Sogang University, Seoul, Korea, where he is currently an associate professor. His research interests are in the areas of mobile wireless transmission, statistical communication theory, distributed antenna systems, and satellite modems.